Optical Engineering

OpticalEngineering.SPIEDigitalLibrary.org

Acousto-optic interaction in biconical tapered fibers: shaping of the stopbands

Gustavo Ramírez-Meléndez
Miguel Ángel Bello-Jiménez
Christian Cuadrado-Laborde
Antonio Díez
José Luis Cruz
Amparo Rodríguez-Cobos
Raúl Balderas-Navarro
Miguel Vicente Andrés Bou

SPIE.

Acousto-optic interaction in biconical tapered fibers: shaping of the stopbands

Gustavo Ramírez-Meléndez,[a] Miguel Ángel Bello-Jiménez,[a,*] Christian Cuadrado-Laborde,[b,c] Antonio Díez,[c] José Luis Cruz,[c] Amparo Rodríguez-Cobos,[a] Raúl Balderas-Navarro,[a] and Miguel Vicente Andrés Bou[c]
[a]Universidad Autónoma de San Luis Potosí, Instituto de Investigación en Comunicación Óptica, Av. Karakorum 1470 Lomas 4a Secc., 78210 San Luis Potosí, S.L.P, México
[b]Instituto de Física Rosario (CONICET-UNR), Optical Metrology Lab, Ocampo y Esmeralda, S2000EZP Rosario, Argentina
[c]Universidad de Valencia, Departamento de Física Aplicada y Electromagnetismo, ICMUV, C/Dr. Moliner 50, Burjassot, 46100 Valencia, Spain

Abstract. The effect of a gradual reduction of the fiber diameter on the acousto-optic (AO) interaction is reported. The experimental and theoretical study of the intermodal coupling induced by a flexural acoustic wave in a biconical tapered fiber shows that it is possible to shape the transmission spectrum, for example, substantially broadening the bandwidth of the resonant couplings. The geometry of the taper transitions can be regarded as an extra degree of freedom to design the AO devices. Optical bandwidths above 45 nm are reported in a tapered fiber with a gradual reduction of the fiber down to 70 μm diameter. The effect of including long taper transition is also reported in a double-tapered structure. A flat attenuation response is reported with 3-dB stopband bandwidth of 34 nm. [DOI: 10.1117/1.OE.55.3.036105]

Keywords: acousto-optic interaction; biconical tapered fiber; acousto-optic filter.

Paper 151598 received Nov. 13, 2015; accepted for publication Feb. 16, 2016; published online Mar. 8, 2016.

1 Introduction

In-fiber acousto-optic (AO) devices based on flexural acoustic waves have been investigated for years because of their applications as frequency shifters,[1] tunable filters,[2] and modulators.[3] Recently, the AO has been investigated as a powerful tool for measuring axial inhomogeneities along optical fibers.[4] When the fundamental flexural acoustic mode propagates along an uncoated single-mode optical fiber (SMF), the acoustic fields produce a periodical perturbation of the fiber, both refractive index changes and geometrical effects, which leads to an intermodal resonant coupling between the fundamental core mode and some specific cladding modes of the SMF.[1–3] This AO interaction can be seen as the dynamic counterpart of a conventional asymmetric long period fiber grating (LPG), whose transmission characteristics can be controlled dynamically by the amplitude and frequency of the acoustic wave. At the output fiber, only the light that remains guided by the core is transmitted, showing a transmittance spectrum with one or several attenuation notches at the wavelengths of the resonant couplings.

The effect of including tapered fibers to improve the AO response has been reported in previous works.[3–8] However, these works paid attention first to the enhancement of the acoustic intensity by reducing the cross section of the fiber and second to the shift of the resonant wavelength in uniform tapered fibers. Thus, the use of a thin optical fiber produces a more efficient intermodal coupling that enables shorter and faster devices, as well as a reduction of the required acoustic power. This fiber tapering can be carried out either by chemical etching or by a fusion and pulling technique.

It is possible to adjust the wavelength of the resonant coupling between two specific modes by changing the frequency of the acoustic wave. However, the spectral bandwidth of a given resonance is determined by the dispersion curves of the involved modes and it is not straightforward how to develop techniques to control such a bandwidth. Kim et al.[9] explored the simultaneous excitation of the acoustic wave generator with two frequencies, while Jung et al.[10] concatenated different fibers. Feced et al.[6] concatenated three fibers with different sections to demonstrate a gain flattening filter and pointed out the interest of exploiting the taper radius as a new degree of freedom in the design of AO filters. Jin et al.[11] demonstrated an enhancement of the bandwidth of the AO notches by using uniform fibers with a reduced diameter prepared with chemical etching. Complimentarily, Li et al.[12] investigated fibers with different dispersion curves in order to narrow the optical notches.

Here, we investigate how tapering can be exploited to control the spectral bandwidth of the transmission notches. It is known that the dispersion curves of both the acoustic and optical modes change with the radius of the fiber.[3] Thus, smooth and long tapered fibers can effectively control the bandwidth of a given coupling by slightly shifting the resonance wavelength, enabling a geometrical design technique, since the shape of fiber tapers can be controlled accurately using a fusion and pulling technique.[13] In Sec. 2, we start with the numerical modeling of acoustically induced LPG formed in a tapered structure. Then, in Sec. 3, we describe the experimental results and the comparison with the theory, in order to demonstrate the effects of the taper transitions on the spectral response of the AO device. Finally, our conclusions are summarized in Sec. 4.

2 Numerical Modeling of the Acousto-Optic Interaction in a Tapered Fiber

In this section, we present the numerical technique that we have implemented to simulate the spectral response of the

*Address all correspondence to: Miguel Ángel Bello-Jiménez, E-mail: m.bello@cactus.iico.uaslp.mx

acoustically induced LPG formed along the device. The intermodal coupling between the core and cladding forward-propagating modes is modeled following the theory developed by Birks et al.[3] The refractive index perturbation, $\Delta n(x,y)$, generated by the acoustic wave is given by the expressions

$$\Delta n(x,y) = \Delta n_0 \sin(\Omega t - Kz), \tag{1}$$

$$\Delta n_0 = n(1-\chi)K^2 u_0 y, \tag{2}$$

where x, y, and z are the Cartesian coordinates, the z axis is the direction of propagation along the fiber for both the light and the acoustic wave, Δn_0 is the perturbation amplitude, n is the refractive index of the fiber glass, χ is the photoelastic coefficient ($\chi = 0.22$ for silica), K is the acoustic wave number, u_0 is the amplitude of vibration of the flexural acoustic wave, which is assumed to vibrate in the direction of the y axis, and Ω is the acoustic wave angular frequency.

The coupling coefficient (κ) between the fundamental mode and a cladding mode is evaluated with the expression

$$\kappa = \frac{\omega}{2c}\iint_A \Delta n_0 \vec{E}_{01}^{*}\vec{E}_{lm}\mathrm{d}x\mathrm{d}y, \tag{3}$$

where ω is the optical angular frequency, c is the speed of light, and E_{lm} is the normalized amplitude of the electric field of a fiber mode, being $l = 0$, $m = 1$ the fundamental mode.

The total optical field is expressed as a superposition of two modes, with amplitudes $A(z)$ and $B(z)$ corresponding to the core and cladding forward-propagating modes, respectively, which satisfy the following pair of coupled-mode equations:

$$\frac{dA(z)}{dz} = -j\kappa B(z)\mathrm{e}^{j\Omega t}\mathrm{e}^{2j\delta z}, \tag{4}$$

$$\frac{dB(z)}{dz} = -j\kappa A(z)\mathrm{e}^{-j\Omega t}\mathrm{e}^{-2j\delta z}, \tag{5}$$

where $j = (-1)^{1/2}$, $\delta = (1/2)(\beta_{01} - \beta_{\mathrm{lm}}) - (\pi/\Lambda)$ is the phase mismatch parameter, β_{01} and β_{lm} being the propagation constants for the fundamental core mode and a high-order cladding mode, respectively, and Λ being the wavelength of the acoustic wave ($K = 2\pi/\Lambda$).

The mode amplitudes, and hence the electric fields, can be readily solved from Eqs. (4) and (5) in terms of a matrix F.[14]

$$\begin{bmatrix} A(z)\mathrm{e}^{-j\beta_{01}z} \\ B(z)\mathrm{e}^{-j\beta_{lm}z} \end{bmatrix} = F \begin{bmatrix} A(0) \\ B(0) \end{bmatrix}, \tag{6}$$

$$F = \begin{bmatrix} \mathrm{e}^{-j\left(\bar{\beta}+\frac{\pi}{\Lambda}\right)z} & 0 \\ 0 & \mathrm{e}^{-j\left(\bar{\beta}-\frac{\pi}{\Lambda}\right)z} \end{bmatrix} \times \begin{bmatrix} \cos(\gamma z) - j\frac{2\delta}{\gamma}\sin(\gamma z), & -\frac{\kappa}{\gamma}\mathrm{e}^{jKz}\sin(\gamma z) \\ \frac{\kappa}{\gamma}\mathrm{e}^{-jKz}\sin(\gamma z) & \cos(\gamma z) + j\frac{2\delta}{\gamma}\sin(\gamma z) \end{bmatrix}, \tag{7}$$

where $\gamma = (\delta^2 + \kappa^2)^{1/2}$, and $\bar{\beta} = (1/2)(\beta_{01} - \beta_{lm})$. The wavelength that satisfies the phase matching condition, i.e., $\delta = 0$, gives the maximum transfer of power and is called the resonant wavelength λ_R.

Then, the taper structure can be modeled by considering an acoustic induced LPG consisting of N cascaded uniform sections with different fiber diameters and lengths L_i. In each section, the local propagation factors of the optical modes will have to be computed. In addition, the acoustic wavelength and amplitude will have to be recalculated for each section since both the velocity, v, and the amplitude of the flexural mode depend on the fiber radius R.

$$v = \sqrt{\pi R c_{\mathrm{ext}} f}, \tag{8}$$

$$u_0(R) = \frac{R}{R_0}u_0(R_0), \tag{9}$$

where c_{ext} is the speed of extensional waves ($c_{\mathrm{ext}} = 5760$ m/s in silica), f is the frequency of the acoustic wave, and R_0 is the original radius of the fiber previous to tapering, and here we have assumed that the acoustic power remains constant along the fiber.

The output from the i'th section becomes the input to the $(i+1)$'th section of the fiber. The output from the N'th section is therefore given by

$$\begin{bmatrix} A(L) \\ B(L) \end{bmatrix} = F_N \cdots F_2 F_1 \begin{bmatrix} A(0) \\ B(0) \end{bmatrix}, \tag{10}$$

where F_i is the F-matrix for the i'th section, as defined by Eq. (7) with $z = L_i$, and $L = \Sigma L_i$ is the total length of the tapered fiber. The lengths L_i were chosen small enough to ensure convergence of the numerical simulations.

Finally, the transmission spectrum of a tapered AO device is modeled by considering that only the fundamental mode is launched into the fiber, i.e., $E_{01}(0) \neq 0$ and $E_{lm}(0) = 0$. Thus, the spectral dependence of the transmittance is obtained by computing $|E_{01}(L)|^2/|E_{lm}(0)|^2$ for each optical wavelength. Previously, the specific cladding mode involved in the experiment will be identified after the theoretical analysis of the phase matching conditions of different cladding modes at the frequency of the acoustic wave.

3 Configuration Under Discussion and Results

A schematic view of the experimental setup is depicted in Fig. 1. The tapered AO device consists of an radio frequency source, a piezoelectric disk (PD), an aluminum horn, and a tapered optical fiber. The fiber is mounted over a metal base and fixed from both ends to avoid being tensioned or relaxed. The PD is excited by the RF source to produce an acoustic wave that is transmitted to the fiber by the aluminum horn.

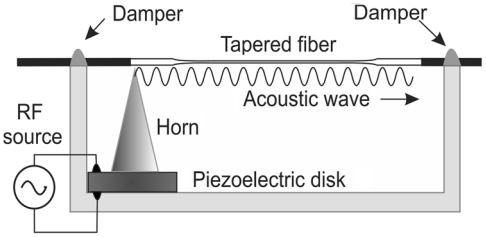

Fig. 1 Experimental setup of the AO device based on a biconical tapered fiber.

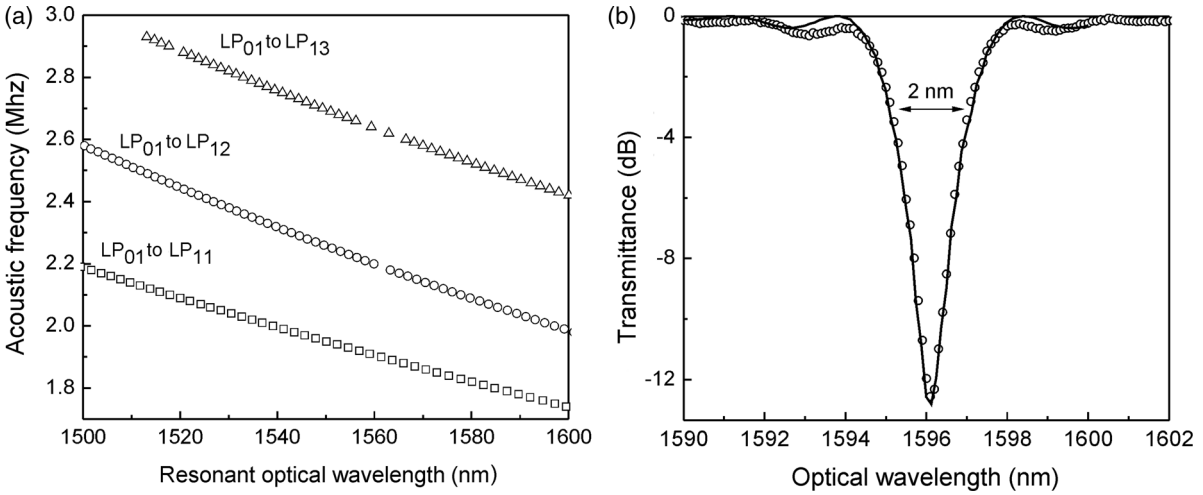

Fig. 2 Theoretical simulation (solid line) and experimental results (scatter points) of the intermodal coupling in a uniform SMF: (a) resonant optical wavelengths and (b) transmittance spectrum at the acoustic frequency of 2.005 MHz.

The horn is attached to the PD, and it focuses the vibration into the fiber through its tip, which is glued to an uncoated optical fiber. The optical fiber was stripped off the outer polymer jacket to prevent the attenuation of the acoustic wave, and the tapered fiber was prepared using a standard fusion and pulling technique to produce a biconical symmetric tapered fiber. In order to prevent acoustic reflections, the acoustic wave is damped in both extremes of the uncoated optical fiber. For the experiments, several fibers were tapered down to diameters of 80, 70, and 65 μm, respectively. In all cases, the total length of the uncoated optical fiber was 24 cm and the tapers had exponential profiles.[13]

At resonance, with a mismatch parameter equal to zero ($\delta = 0$), λ_R has an explicit dependence on the root square of the fiber radius R, expressed by the following relation:

$$\lambda_R = (n_{01} - n_{lm})\sqrt{\frac{\pi\, C_{\text{ext}}\, R}{f}}, \tag{11}$$

where n_{01} and n_{lm} are the modal refractive indexes of the fundamental core mode and a cladding mode ($n_{01} = \beta_{01}/k_0$ and $n_{lm} = \beta_{lm}/k_0, k_0 = 2\pi/\lambda$), respectively. As it can be seen from Eq. (11), a small variation in R will produce a shift of the resonant optical wavelength. Consequently, the reduction of the fiber diameter along the taper will produce a gradual shift of the resonant optical wavelength, which will contribute to broadening the spectral response of the acoustically induced LPG, in addition to the broadening produced by the reduced diameter of the uniform taper waist. Because of the gradual confinement of the acoustic wave along the tapered fiber, a stronger AO effect is also expected, which leads to a more efficient intermodal coupling.

In the experiments commercially available Corning LEAF fiber was used to prepare the tapered fibers and to implement the AO devices.

3.1 *Acousto-Optic Interaction in a Single-Mode Optical Fiber and Simulation Parameters*

The first set of experiments was intended to obtain the flexural wave frequencies, which satisfy the phase-matching condition between the fundamental core mode LP_{01} and some specific higher-order cladding mode LP_{1m}. This experimental information will permit the identification of the cladding mode excited in the experiments and a fine adjustment of the fiber parameters in order to ensure that the theoretical model correctly simulates the fiber. The experimental scheme is the same as that shown in Fig. 1, but using a 24 cm long nontapered single-mode fiber. The AO resonances and the spectral response were measured using an erbium broadband amplified spontaneous emission light source and an optical spectrum analyzer with 30 pm resolution. Experimental results of the AO resonances are shown in Fig. 2(a) for a range of optical wavelengths between 1500 and 1600 nm. Working in the frequency range from 1.7 to 3 MHz, LP_{01} to LP_{11}, LP_{01} to LP_{12}, and LP_{01} to LP_{13} intermodal couplings were observed. For the specific fiber of our experiments, the strongest mode-coupling was found at the acoustic frequency of 2.005 MHz, corresponding to the modes LP_{01} to LP_{12}. The spectral dependence of its transmittance is shown in Fig. 2(b). It exhibits a maximum rejection efficiency of 12.8 dB at the optical resonant wavelength of 1596 nm, and a 3-dB stopband bandwidth of 2 nm. The width of the stopband is determined at the point where the transmission response drops by 3 dB.

After computing the modal indexes of the fundamental and high-order cladding modes using a standard boundary-value

Table 1 Simulation parameters used in the numerical computation.

	Corning LEAF fiber (datasheet)	Simulation parameters
Cladding diameter	125 ± 0.7 μm	125 μm
Mode field diameter	9.6 ± 0.4 μm	11.66 μm
Numerical aperture at 1550 nm	0.14 (typical value)	0.1074
Effective area at 1550 nm	72 μm^2	106.8 μm^2
Effective group index at 1550 nm	1.468	1.466
Core diameter	—	9.3 μm

Table 2 Parameters of the tapered optical fibers.

Waist diameter (μm)	Transition length (cm)	Waist length (cm)	Acoustic frequency (MHz)	3-dB stopband bandwidth (nm)
Nontapered single-mode fiber (125 μm)	—	24.0	2.005	2
80	5.06	11.0	0.540	9.2
70	5.90	10.0	1.194	45
65	5.98	9.0	1.207	34

method, applied to a step index fiber, the resonant optical wavelengths for a given acoustic frequency f were calculated from Eq. (11). Material dispersion of the optical fiber was estimated considering Sellmeier coefficients of a binary silica glass doped with GeO_2 in the core, and pure silica glass in the cladding.[15,16] The experimental results were best fitted with a GeO_2 concentration of ~3.1%, maintaining the core radius at a constant 9.3 μm. Table 1 gives the actual values of the simulation parameters, together with the nominal values provided by the fiber manufacturer. Simulation parameters were calculated to be closest to the LEAF fiber datasheet.

3.2 *Acousto-Optic Interaction in a Biconical Tapered Fiber*

We focus our attention on the effects of large taper transitions as a mechanism to shape the transmission spectrum, for example, to increase the optical bandwidth of the AO stopbands. The tapered fibers were prepared using a standard fusion and pulling technique, and were tapered down to a fiber diameter of 80, 70, and 65 μm, respectively. In this process, both the core and cladding diameters are reduced simultaneously, providing an increase of the intensity of the acoustic wave and the coupling coefficient (due to the mode field diameter increases). The fiber tapers are composed of relatively long decaying exponential profiles with a uniform taper waist. For these particular cases, the taper structures were prepared to produce a spectral response that is dependent on the taper transition. The parameters of the fiber tapers are depicted in Table 2.

The transmission spectra of the acoustically induced LPG are shown in Fig. 3 for the 80, 70, and 65 μm fiber tapers. The acoustic frequency was selected to produce the maximum transfer of energy, around 1550 nm, and that corresponded to 0.540, 1.194, and 1.207 MHz for the three tapers of 80, 70, and 65 μm, respectively. The maximum rejection efficiencies produced by these tapers were 18, 6.2, and 4 dB, respectively. Numerical simulations of the spectral response are also shown in Figs. 3(a)–3(c).

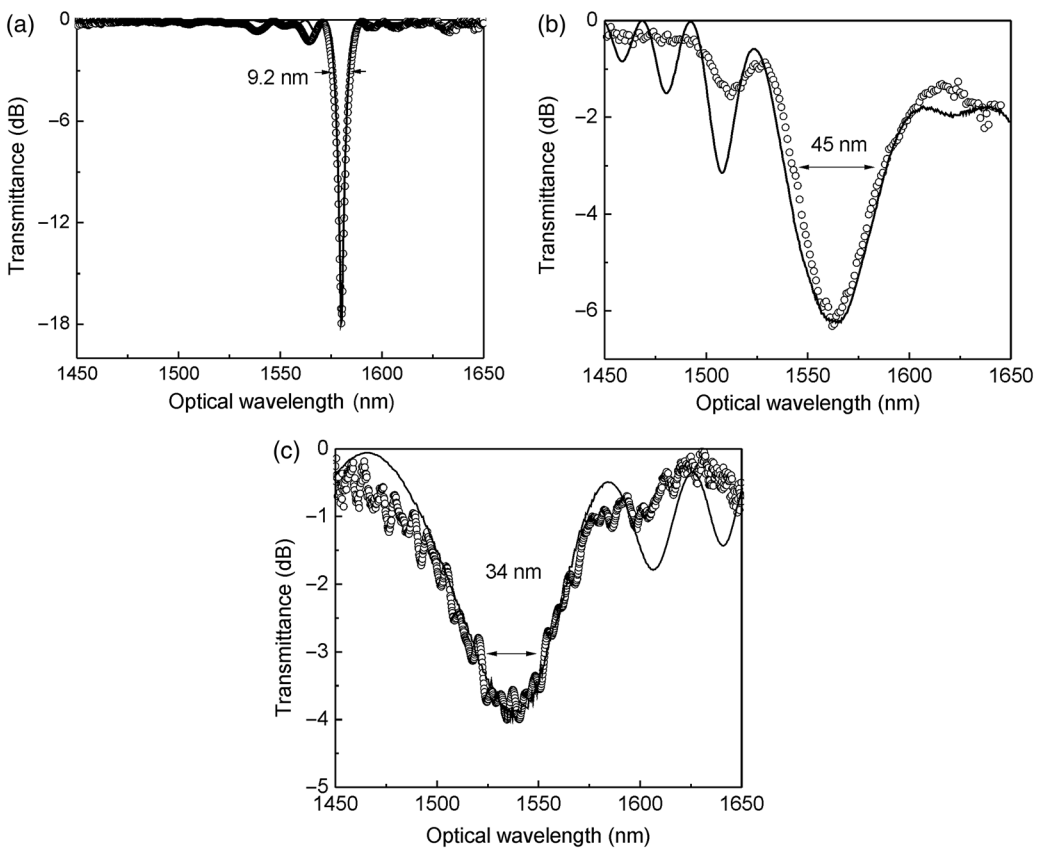

Fig. 3 Transmission spectra for three different tapered fibers at different acoustic frequencies: (a) 80 μm, (b) 70 μm, and (c) 65 μm waist diameters. In all cases, simulations are shown as solid curves and experimental values as scatter points. Arrows indicate the 3-dB stopband bandwidth.

From these results, an increment of the notch bandwidth that is dependent on the reduction of fiber diameter can be observed. In our experiments, the bandwidth increases from 9 to 45 nm when the waist diameter is reduced from 80 to 70 μm, respectively, and then, the bandwidth is reduced to 34 nm for the device with 65 μm waist diameter. This reduction in bandwidth can be attributed to the spectral contributions of the taper waist and the taper transitions. For the 70 μm taper, both the waist and transitions have a similar resonant optical wavelength, contributing to produce a broad spectral response. If we compare these values with the spectral response of a nontapered single-mode fiber [2 nm of 3-dB stopband bandwidth for a fiber diameter of 125 μm, see Fig. 2(b)], we can appreciate a 4.5× to a 22.5× improvement in the optical bandwidth achieved with the present approach.

From Fig. 3, we can conclude that our numerical simulations are realistic, so we can use the simulation tool to gain insight into the AO interaction along the device. Thus, we have separately computed the contributions of isolated transitions and waist. Figure 4 shows numerical simulations of the spectral response for the taper waist and the two taper transitions for the three tapered fibers of the experiments. First, we can see that for the relatively large waist diameter, the device with 80 μm diameter in Fig. 4(a), the largest contribution comes from the waist region of the device. Then, for the device with 70 μm waist diameter in Fig. 4(b), we can observe that the broadening of the notch is enhanced simultaneously by the contribution of both the taper waist and the taper transitions. Finally, for the device with 65 μm waist diameter [Fig. 4(c)], the role of the taper transitions is the dominant one to produce the spectral broadening.

Computed results demonstrate that taper transitions can play an important role to improve the optical bandwidth of the AO stopbands. The main contribution of taper transitions can be obtained when both the taper waist and the taper transitions have a similar resonant optical wavelength, contributing simultaneously to shape the transmittance spectrum of the device. We should also comment that the final transmittance of the device is not the simple addition of the transmittance of isolated sections, since a proper concatenation of the sections takes into account the amount of power already coupled in the previous sections and the phase accumulated in each mode.

3.3 *Acousto-Optic Interaction in a Complex Tapered Structure*

In Sec. 3.2, it was shown that the gradual variation of the taper transition gives rise to a local and broad AO resonance that can be used to improve the optical bandwidth of the AO stopbands. One important application of this AO interaction

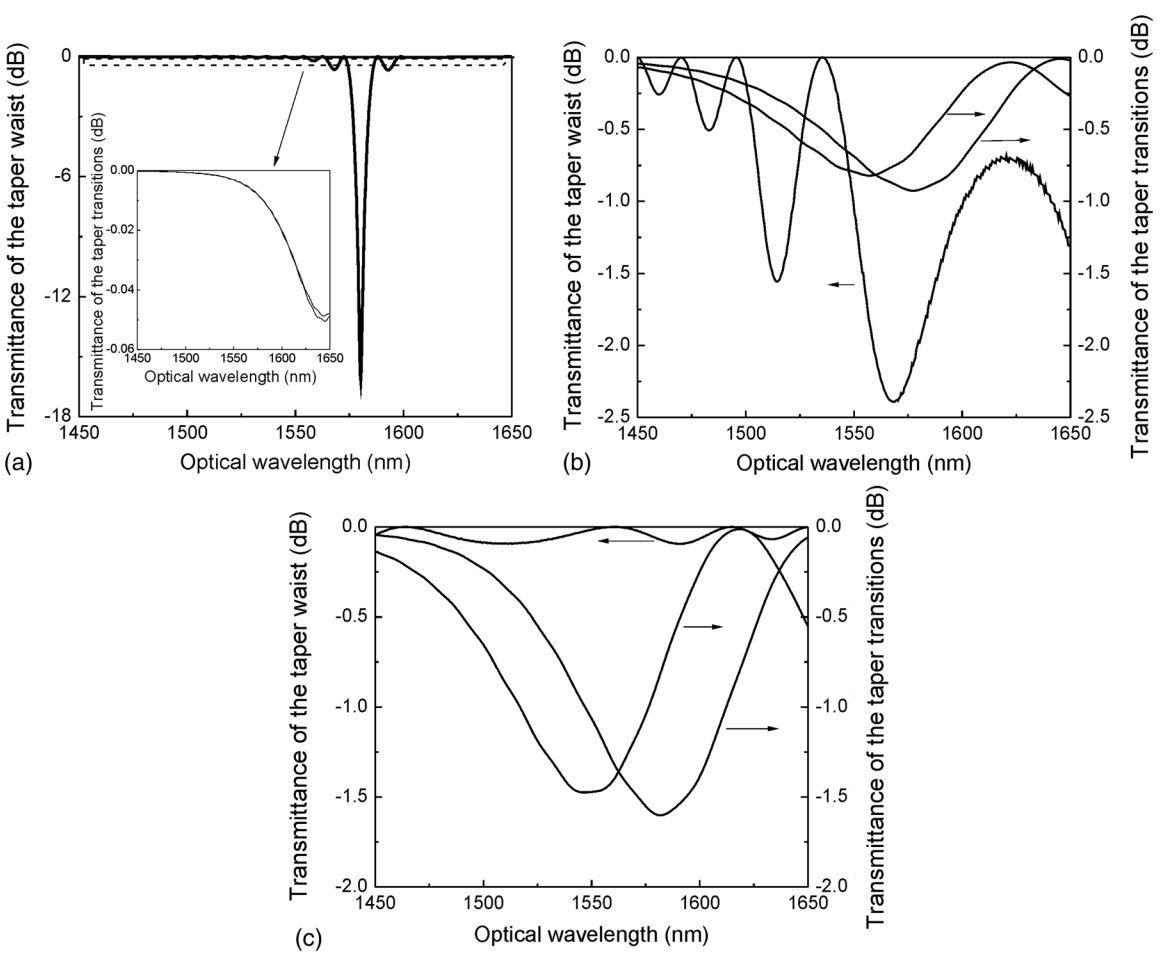

Fig. 4 Numerical simulations of the spectral response considering the taper transitions and the taper waist as independent parts in the tapered fibers of (a) 80 μm, (b) 70 μm, and (c) 65 μm, respectively. The inset in Fig. 4(a) shows a zoom view of the spectral response for the transitions.

can be found in the development of broad-bandwidth AO modulators, with applications in actively mode-locked fiber lasers.[17,18] In this section, we will discuss a design consisting of two cascaded tapered fiber, which enables a broad and flat spectral response and also shows other interesting features that can be achieved. Our purpose is to demonstrate that the geometry of the taper transitions can be regarded as an extra degree of freedom for the design of AO devices.

For this purpose, a set of theoretical simulations are depicted in Figs. 5(a)–5(d) to obtain an insight into the AO interaction in a tapered structure. Figure 5(a) shows the relation between the acoustic wave frequency (f_a) and the fiber waist diameter for the LP_{01} to LP_{11}, LP_{01} to LP_{12}, and LP_{01} to LP_{13} intermodal couplings to obtain a resonance optical wavelength (λ_R) at 1550 nm. Figure 5(b) shows the relation between f_a and the resonant optical wavelength in a range from 1450 to 1650 nm for the 125 to 65 μm and 65 to 125 μm taper transitions; the inset shows the transmittance spectrum of the taper transition. For estimating purposes, Fig. 5(c) depicts the relation between the 3-dB stopband

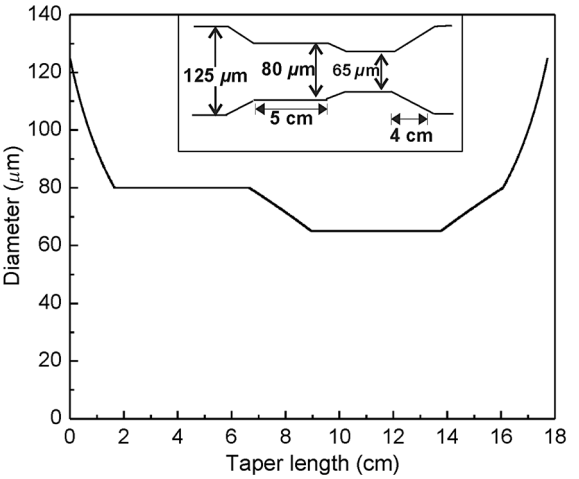

Fig. 6 Geometrical shape of the double-tapered structure. Inset shows a more detailed representation of the structure dimensions.

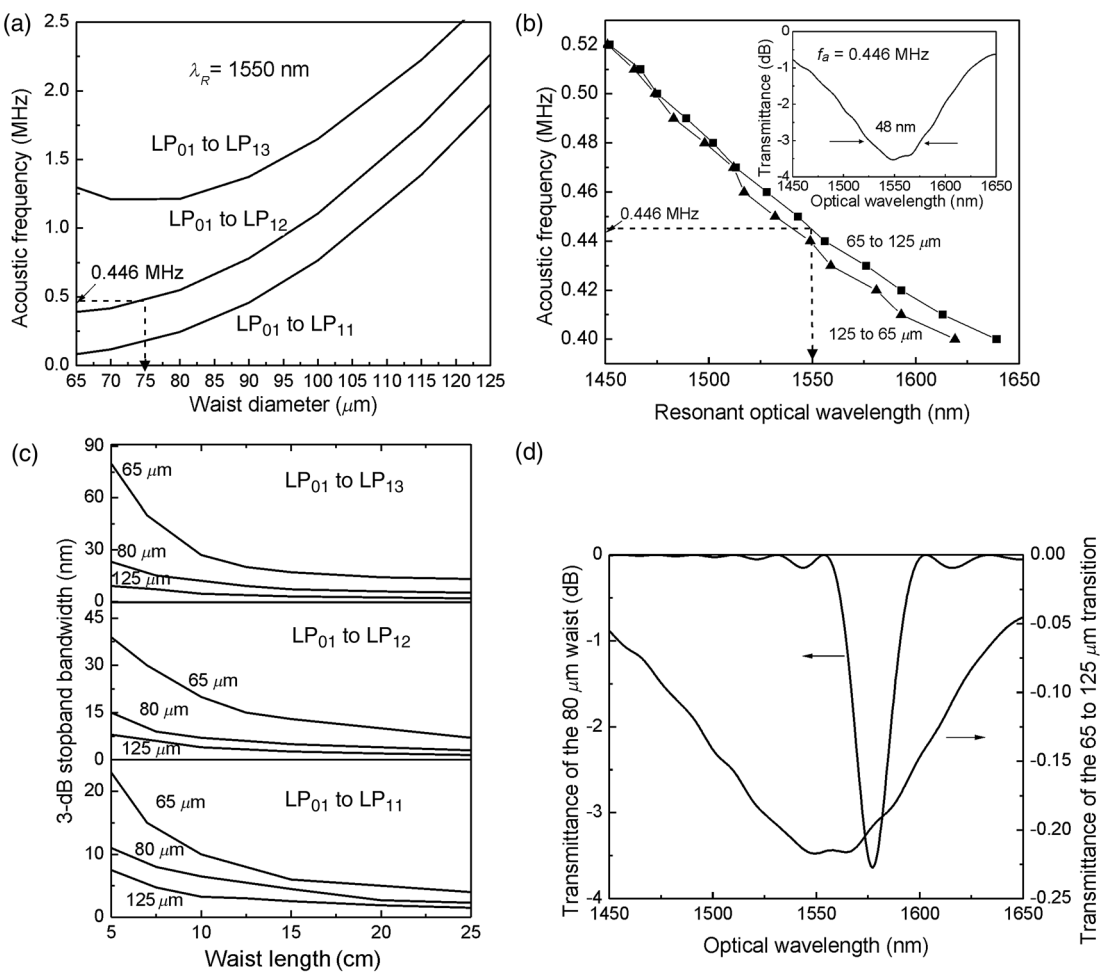

Fig. 5 Numerical simulation of AO resonances. (a) Relation between acoustic wave frequency (f_a) and the fiber waist diameter for the LP_{01} to LP_{11}, LP_{12}, and LP_{13} resonances. (b) Relation between f_a and the resonant optical wavelength for the 125 to 65 μm and 65 to 125 μm taper transitions; the inset shows the transmittance spectrum of the taper transition. (c) 3-dB stopband bandwidth as a function of the waist length. (d) Spectral response for a 5-cm-long uniform taper waist of 80 μm diameter and a 4-cm-long taper transition.

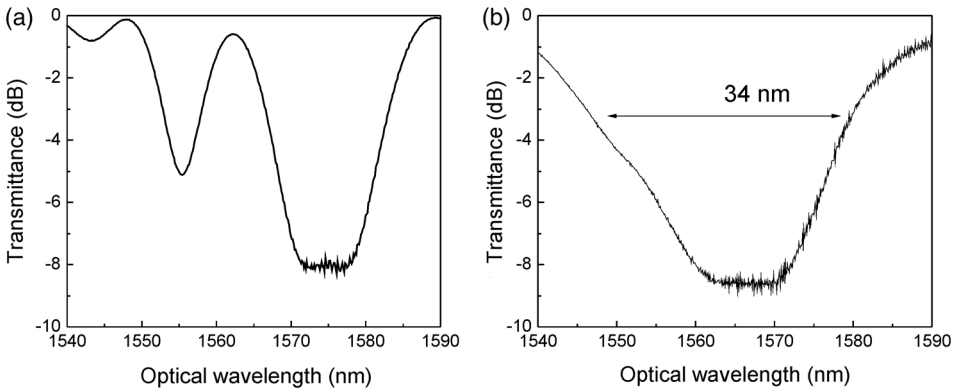

Fig. 7 Flat attenuation notch produced by the contribution of both the taper waist (80 μm) and the taper transition (65 to 125 μm): (a) simulation and (b) experimental result.

bandwidth and the waist length for the LP_{01} to LP_{11}, LP_{12}, and LP_{13} resonances. From these results, it can be observed that an acoustic frequency of 0.446 MHz produces the same AO resonance ($\lambda_R = 1550$ nm) for a 75 μm waist diameter and a 65 to 125 μm taper transition. In order to shape the spectral response, we simulated the AO interaction in a waist and a taper transition whose transmittance spectra were near each other in resonant wavelengths. Figure 5(d) shows the spectral response for a 5-cm-long uniform taper waist of 80 μm diameter and a 4-cm-long taper transition, from 65 to 125 μm in diameter, both of them simulated at the acoustic frequency of 0.446 MHz. The resonant optical wavelengths for each component were 1576 and 1550 nm, respectively.

The device that combines here two responses comprises two cascaded tapered fibers. The first taper is prepared to produce an 80 μm uniform taper waist of a length of 5 cm. Then, a second taper is realized at one end of the uniform waist to produce a second tapered structure with a uniform section of 65 μm. Due to the fabrication procedure, the taper profile includes a relatively long transition region of a length of 4 cm, with a diameter variation from 65 to 125 μm. In order to shape the spectral response by the uniform 80 μm waist region and the long taper transition, the AO attenuator is driven with a frequency close to 0.446 MHz. The geometrical shape of the tapered structure is depicted in Fig. 6. The characteristics of taper waist and transitions are estimated with a well-established model for fiber tapers.[13]

Experimentally, the best result was found at the acoustic wave frequency of 0.47 MHz. This frequency was selected to shape the spectral response by the contribution of both the uniform 80 μm waist region and the long taper transition (65 to 125 μm). Figure 7 shows the simulated and experimental transmittance spectra of the AO device. As it can be observed, the device exhibits an almost flat attenuation response, with a maximum rejection efficiency of 8.5 dB, from 1562 to 1570 nm, centered at the optical resonant wavelength of 1566 nm, and a 3-dB stopband bandwidth of 34 nm. In addition, the "red" side of the attenuation dip exhibits a high slope, since the slopes of both the responses of the 80 μm section and the 65 to 125 μm tapered section match each other (see Fig. 5). On the other hand, at the "blue" side of the attenuation dip, the slope is smooth, since the two contributions depicted in Fig. 5 are shifted. As a result, with this specific device, we show the possibility of broadening the attenuation dip and shaping it in order to produce sharper or smoother quasilinear spectral response at specific wavelength ranges.

4 Conclusions

Our experiments and simulations demonstrate that biconical tapered fibers can be designed to increase the bandwidth of the AO stopbands and to shape the spectral response. The good agreement between experiments and theory enables the use of our simulation tool for the design of devices with a specific response. From experimental results, we can conclude that geometry of the taper transitions can be regarded as an extra degree of freedom to the design of AO devices. Optical bandwidths above 45 nm are reported in a tapered fiber with a gradual reduction of the fiber down to 70 μm diameter. As a special case, a double-tapered structure was designed in order to obtain a flat bottom spectral response and asymmetric sides.

Acknowledgments

This investigation has been financially supported by CONACyT grants 206425 and 222476, and Promep DSA/103.5/14/10476.

References

1. B. Y. Kim et al., "All-fiber acousto-optic frequency shifter," *Opt. Lett.* **11**(6), 389–391 (1986).
2. D. Östling and H. E. Engan, "Narrow-band acousto-optic tunable filtering in a two-mode fiber," *Opt. Lett.* **20**(11), 1247–1249 (1995).
3. T. A. Birks, P. S. J. Russell, and D. O. Culverhouse, "The acousto-optic effect in single-mode fiber tapers and couplers," *J. Lightwave Technol.* **14**(11), 2519–2529 (1996).
4. E. P. Alcusa-Sáez et al., "Improved time-resolved acousto-optic technique for optical fiber analysis of axial non-uniformities by using edge interrogation," *Opt. Express* **23**(6), 7345–7356 (2015).
5. T. A. Birks, P. S. J. Russell, and C. N. Pannell, "Low power acousto-optic device based on a tapered single-mode fiber," *IEEE Photonics Technol. Lett.* **6**(6), 725–727 (1994).
6. R. Feced et al., "Acoustooptic attenuation filters based on tapered optical fibers," *IEEE J. Sel. Top. Quantum Electron.* **5**(5), 1278–1288 (1999).
7. Q. Li et al., "Highly efficient acoustooptic tunable filter based on cladding etched single-mode fiber," *IEEE Photonics Technol. Lett.* **14**(3), 337–339 (2002).
8. F. Abrishamian et al., "Design theory and experiment of acousto-optical tunable filter by use of flexural waves applied to thin optical fibers," *Opt. Quantum Electron.* **40**(9), 665–676 (2008).
9. H. S. Kim et al., "All-fiber acousto-optic tunable notch filter with electronically controllable spectral profile," *Opt. Lett.* **22**(19), 1476–1478 (1997).
10. Y. Jung et al., "Bandwidth control in a hybrid fiber acousto-optic filter," *Opt. Lett.* **30**(1), 84–86 (2005).

11. T. Jin et al., "Ultra-broad-band AOTF based on cladding etched single-mode fiber," *IEEE Photonics Technol. Lett.* **14**(8), 1133–1335 (2002).
12. Q. Li, X. Liu, and H. P. Lee, "Demonstration of narrow-band acousto-optic tunable filters on dispersion- enhanced single-mode fibers," *IEEE Photonics Technol. Lett.* **14**(11), 1551–1553 (2002).
13. T. A. Birks and Y. W. Li, "The shape of fiber tapers," *J. Lightwave Technol.* **10**(4), 432–438 (1992).
14. T. Erdogan, "Fiber gratin spectra," *J. Lightwave Technol.* **15**(8), 1277–1294 (1997).
15. H. Jeong and K. Oh, "Theoretical analysis of cladding-mode waveguide dispersion and its effects on the spectra of long-period fiber gratings," *J. Lightwave Technol.* **21**(8), 1838–1845 (2003).
16. J. W. Fleming, "Material dispersion in lightguide glasses," *Electron. Lett.* **14**(11), 326–328 (1978).
17. M. Bello-Jiménez et al., "Actively mode-locked fiber ring laser by intermodal acousto-optic modulation," *Opt. Lett.* **35**(22), 3781–3783 (2010).
18. M. Bello-Jiménez et al., "Mode-locked all-fiber ring laser based on broad bandwidth in-fiber acousto-optic modulator," *Appl. Phys. B* **110**(1), 73–80 (2013).

Gustavo Ramírez-Meléndez received his MSc degree in electrical engineering from the Universidad Autónoma de San Luis Potosí (UASLP). He is currently pursuing his PhD in applied sciences with the Instituto de Investigación en Comunicación Óptica, UASLP. His research interests include the acousto-optic interaction in optical fibers and the development of optical fiber devices.

Miguel Ángel Bello-Jiménez received his PhD in optics from the National Institute for Astrophysics, Optics and Electronics, Puebla, México, in 2010. He joined the Departamento de Física Aplicada y Electromagnetismo, Universidad de Valencia, Spain, two years ago. He is currently a professor/researcher at the Instituto de Investigación en Comunicación Óptica, UASLP. His current research interests include nonlinear effects, fiber optics, and fiber lasers.

Christian Cuadrado-Laborde received his PhD in physics from the National University of La Plata, Buenos Aires, Argentina, in 2005. He was awarded by the Spanish Ministry of Science with a research fellow position to join the Optical Fiber Laboratory group of the University of Valencia, during 2008 to 2009. His current research interests include photonics, signal processing, fiber optics applications, and fiber lasers.

Antonio Díez received his PhD in physics in 1998 from the University of Valencia. In 1999, he joined the Optoelectronics Research Group at the University of Bath for two years. Currently, he is a profesor titular de universidad in the Departamento de Física Aplicada y Electromagnetismo at the Universidad de Valencia, Spain. His current research interests include photonic crystal fibers, fiber lasers, optical microresonators, and optical sensors.

José Luis Cruz received his PhD in physics from the University of Valencia in 1992. Since 1995, he has been a staff member of the Applied Physics Department at the University of Valencia. He is a coinventor of six patents and coauthor of 130 papers in international journals. He is a member of OSA. He is a permanent professor and vice dean of the physics faculty.

Amparo Rodríguez-Cobos received her PhD in optoelectronics from the Institut National Polytechnique de Grenoble, Grenoble, France, in 2001. Since 2002, she has been a professor and researcher at the Instituto de Investigación en Comunicación Óptica, UASLP. Her research interests include the development of integrated optics devices, the applications of fiber optics devices, and the technological application of photochromic polymer films.

Raúl Balderas-Navarro received his PhD in applied physics from UASLP in 1998. Currently, he is a profesor-investigador at the Instituto de Investigación en Comunicación Óptica in UASLP. His current research interests include optical processes in semiconductors.

Miguel Vicente Andrés Bou received his doctor en física degree from the Universidad de Valencia in 1985. He founded the Optical Fiber Laboratory Group, Universidad de Valencia, in 1987. His current research interests include waveguide theory (photonic crystal fibers and inhomogeneous waveguides), optical fiber devices, systems for microwave photonics, all-fiber lasers (active Q-switched and mode-locked fiber lasers), and sensors.